

Co-option of the piRNA pathway for germline-specific alternative splicing of *C. elegans*

TOR

Sergio Barberán-Soler, Laura Fontrodona, Anna Ribó, Ayelet T. Lamm, Camilla Iannone, Julián Cerón, Ben

Lehner, Juan Valcárcel

Supplementary Materials

Figures S1-S4

Table S1

Materials and Methods

References (1-7)

Supplementary Figures

Figure S1

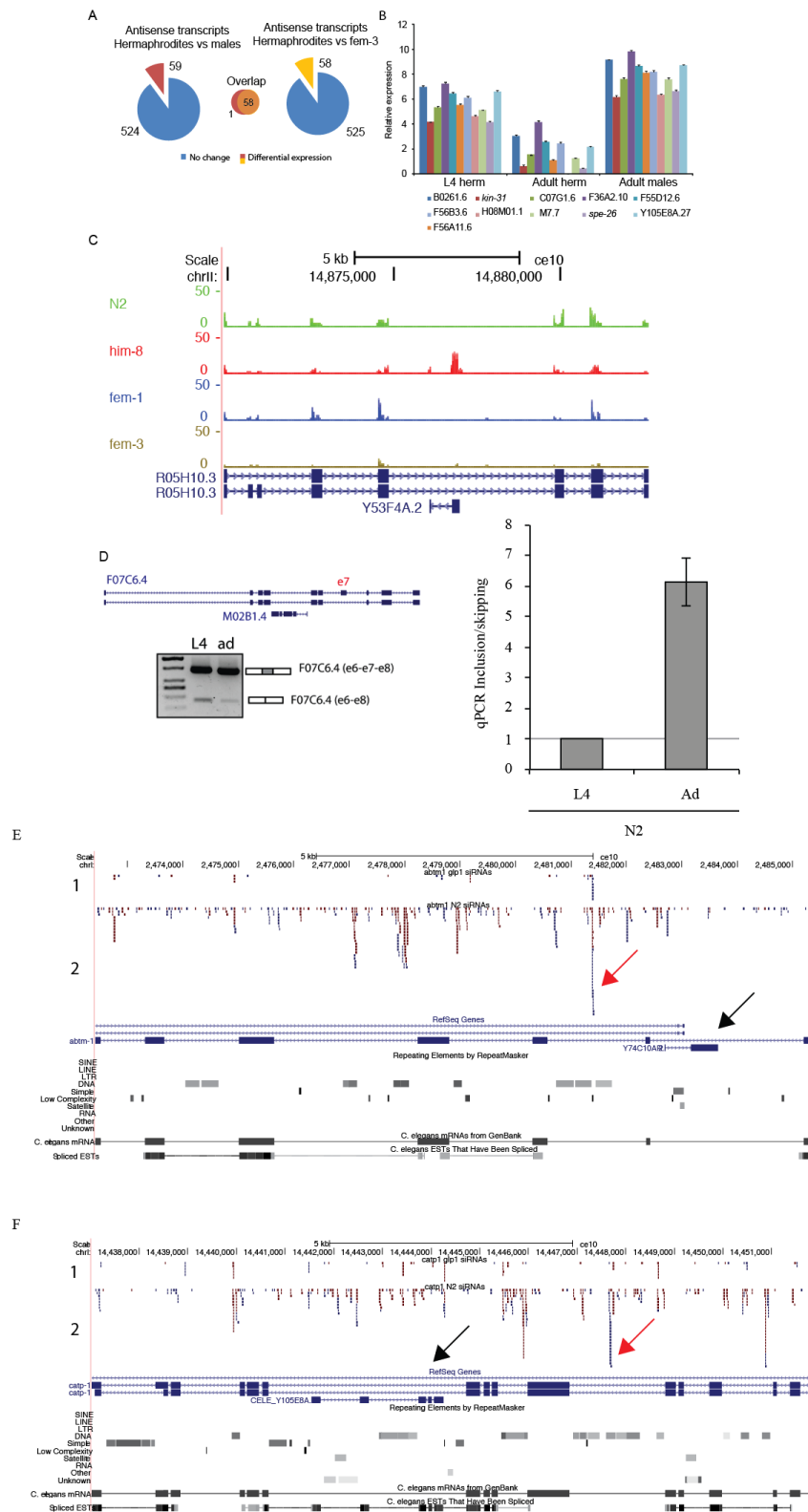


Figure S1. *C. elegans* sperm-specific antisense transcripts and associated endo-siRNAs (related to Figure 1). **A) Identification of 58 sperm-specific antisense transcripts.** Differentially expressed antisense transcripts identified from mRNA-Seq data. The chart on the left shows the number of antisense transcripts with differential expression between adult hermaphrodites and adult males; the chart on the right shows the number of antisense transcripts that are differentially expressed between adult hermaphrodites (wild type) and mutant hermaphrodites that just produce sperm cells; the chart in the center shows the overlap between differentially expressed antisense transcripts in the other two charts; **B) RT-qPCR validation of sperm-specific expression of 9 antisense transcripts selected at random.** The expression values of each antisense transcript were normalized to housekeeping genes (*rsp-1* and *gpd-2*), the samples used are wild-type L4 worms (undergoing spermatogenesis), wild-type adult hermaphrodites (undergoing oogenesis) and adult males (purified from a *him-8(e1489)* population, see methods); error bars indicate the standard deviation; **C) An example of a sense/antisense pair.** Genome browser display of R05H10.3 and its sperm-specific antisense transcript Y53F4A.2 (similar to Figure 1A). **D) F07C6.4 alternative splicing regulation during development.** Left panel and gel, F07C6.4 gene model and alternative splicing regulation between L4 and adult WT worms detected by semiquantitative RT-PCR; right panel, RT-qPCR of F07C6.4 exon 7 splicing between L4 and adult WT worms, ratio of inclusion/skipping quantified by RT-qPCR. **E, F) Examples of endo-siRNAs aligned to transcriptional units displaying alternative splicing events and harboring male germline-specific antisense transcripts.** Displays are represented as in Figure 1C. E) *abtm-1* and F) *catp-1*; sRNA reads for *glp-1* germline-less worms are on track 1, for wild-type L4 worms on track 2, regions of

antisense transcription are indicated by a black arrow. Regions of abundant endo-sRNAs are indicated by red arrows.

Figure S2

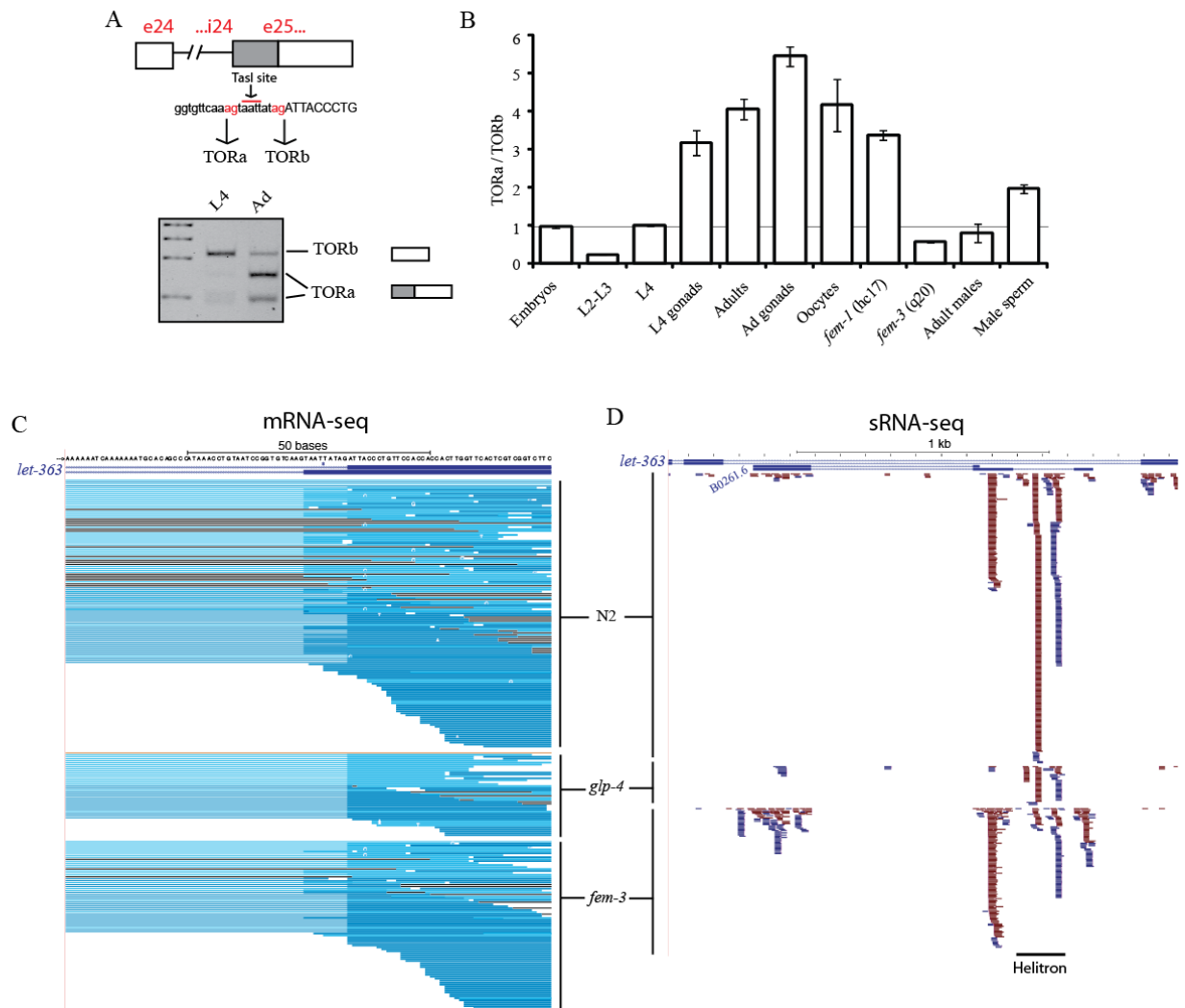


Figure S2. *CeTOR* (*let-363*) alternative splicing regulation and associated endo-siRNAs (related to Figure 2). A) Changes in *TOR a/b* isoform ratios during development and gonad formation. *CeTOR* alternatively spliced region involves two alternative 3' splice sites separated by 9 nucleotides (corresponding to protein variants differing by 3 amino acids). Bottom panel: semiquantitative-RT-PCR analysis of RNA from L4 and adult worms using primers in exons 24 and 25 flanking the alternative exon junctions; amplification products were digested with *TasI*

(recognition site indicated in the upper panel) and separated by gel electrophoresis. The positions of fragments corresponding to the *CeTOR* a and b isoforms are indicated; **B) Ratio between *CeTOR*a and b isoforms obtained by RT-qPCR analysis of RNA from worms of different sex, developmental stages and organs;** ratios are normalized to the values obtained for L4 whole worms. Error bars correspond to standard deviations of at least three biological replicates, with three technical qPCR replicates each. **C) Changes in *TOR* a/b ratio detected by mRNA Seq.** Genome browser shot of *CeTOR* alternatively spliced region in intron 24. The two alternative 3' splice sites and the following exonic sequences are indicated by blue thick bars. Tracks display mRNA-Seq reads obtained from N2, *glp-4* and *fem-3* adult worms. The reads detect approximately 50% of use of each isoform in N2 worms, 25% of a isoform in *fem-3* worms and no evidence of a isoform in *glp-4* (germline-less) worms. **D) Endo-siRNAs detected in *CeTOR* intron 21 by sRNA-Seq.** Genome browser shot of intron 21 of *CeTOR* including the antisense transcript B0261.6; the tracks display sRNA-seq reads obtained from the same biological samples as A). sRNAs corresponding to regions of *CeTOR* / B0261.6 overlap are abundant in N2 and *fem-3* worms but much less abundant in *glp-4* worms.

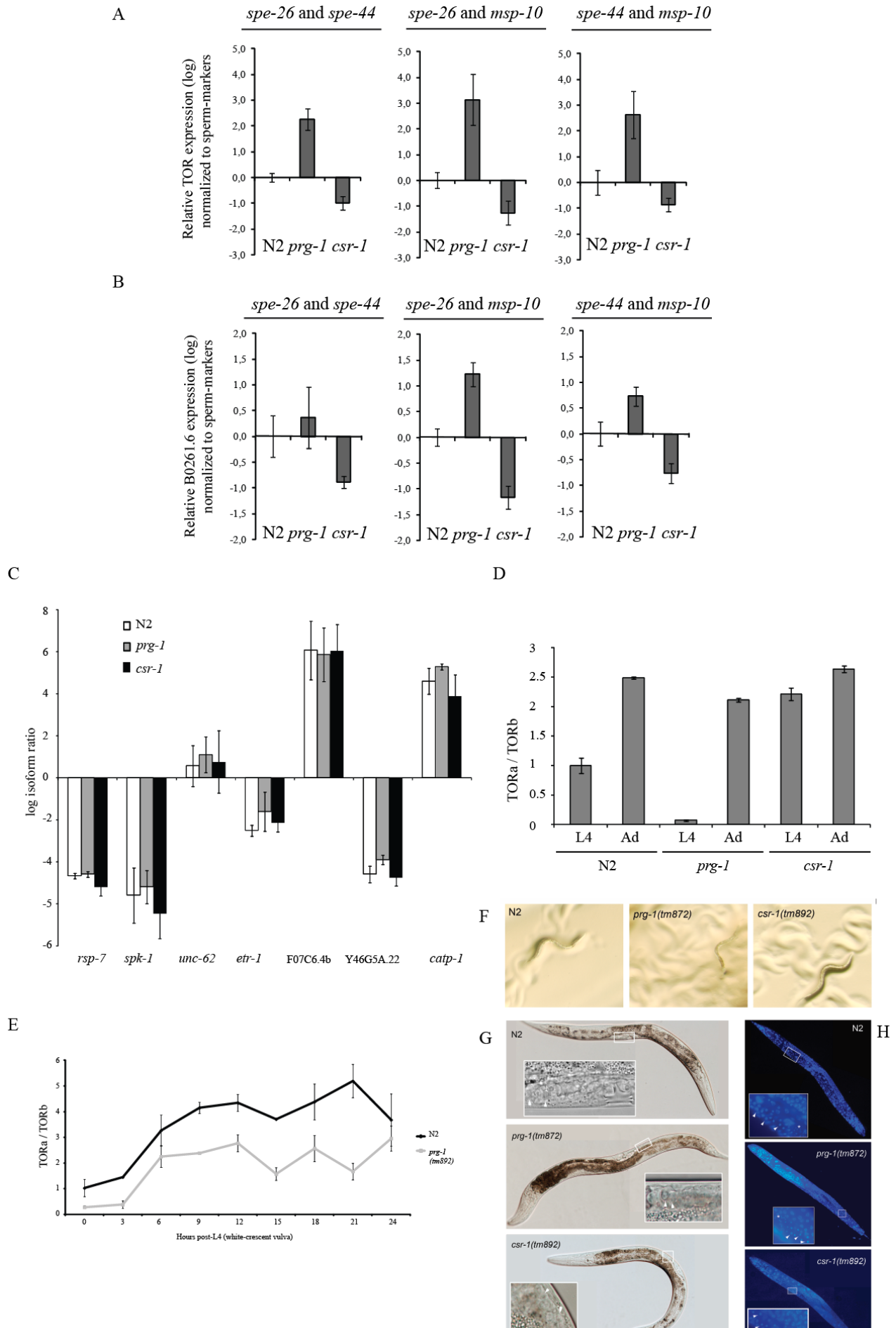
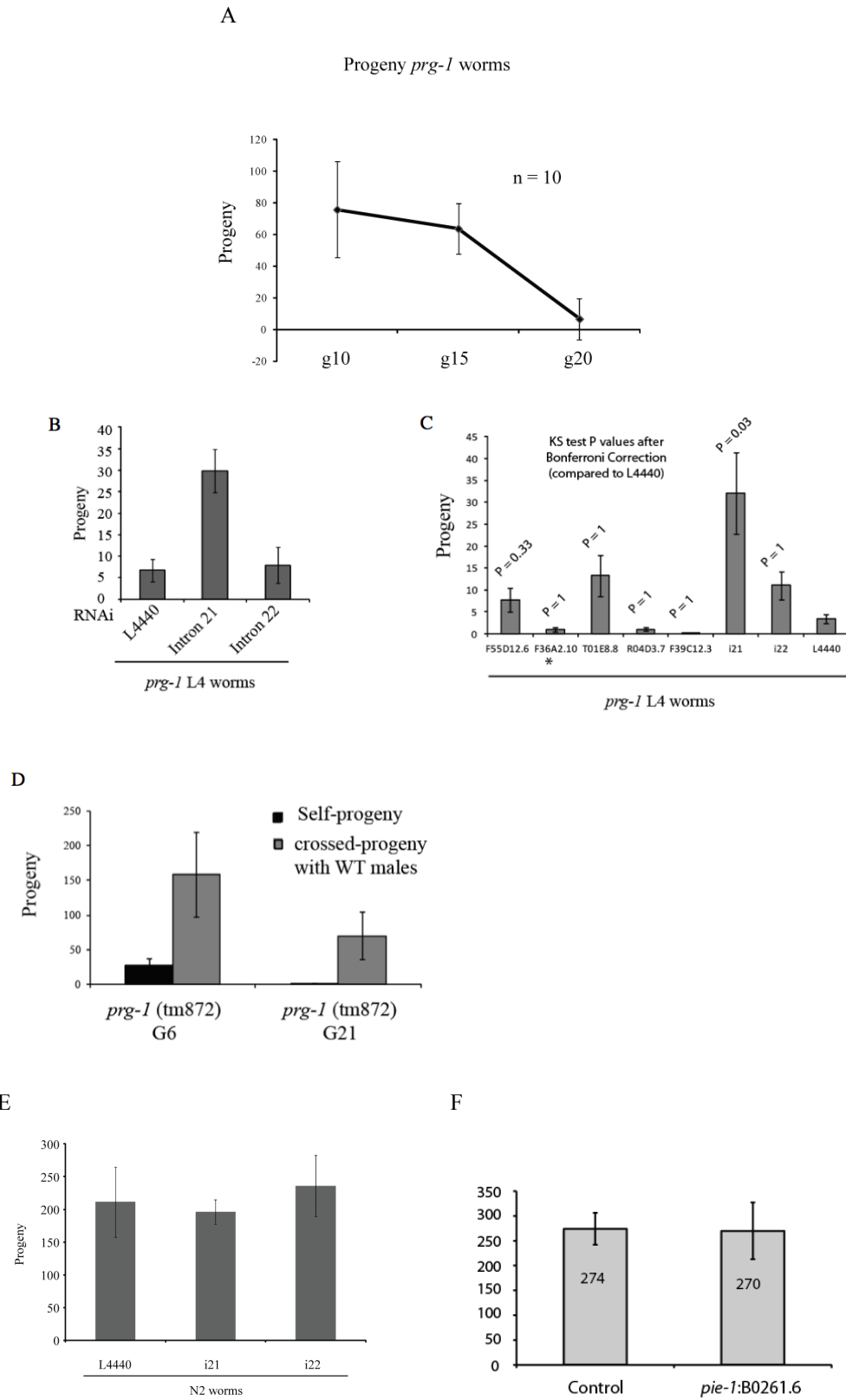


Figure S3. Regulation of *CeTOR* alternative splicing by *prg-1* and *csr-1* (related to Figure 4). **A, B) Expression of B0261.6 and *CeTOR* in wild type and mutants worms using different subsets of male germline-specific markers for normalization.** This normalization serves to account for possible reductions in the male germline in mutants of Argonaute proteins *prg-1* and *csr-1*. Expression values of test genes and markers were obtained by RT-qPCR and every possible pair of *spe-26*, *spe-44* and *msp-10* male germline-specific markers was used for normalization, as in Figure 4 and as explained in Methods. Consistent results for changes in expression of B0261.6 and *CeTOR* were obtained in all conditions. Error bars indicate the standard deviation. **C) Alternative splicing of genes abundant in germline tissues is not affected in *prg-1* or *csr-1* mutant worms.** Seven genes with differential expression between sex-specific samples and with alternative splicing events that show regulation between sex-specific samples were assayed by RT-qPCR to obtain ratios between alternatively spliced RNA isoform in N2, *prg-1* and *csr-1* worms. Error bars represent standard deviation from three biological replicas. We conclude that neither *prg-1* nor *csr-1* mutations cause general changes in alternative splicing. **D) Mutation of *prg-1* and *csr-1* affect *CeTOR* alternative splicing of hermaphrodite L4 worms but not of adult worms.** Ratios between *CeTOR* splicing isoforms were determined by RT-qPCR and in Figure 4D for L4 or adult (Ad) worms, either wild type (N2) or *prg-1* or *csr-1* mutants. The results show a reduction of the *CeTORa/b* ratio in *prg-1* mutants and an increase in *csr-1* mutants in L4 hermaphrodite worms, but no significant differences in adult animals. Error bars indicate standard deviation. **E) N2 and *prg-1* worms have different TOR isoform ratios throughout the L4 to adult transition.** N2 and *prg-1* worms were synchronized at the L4 stage, samples were collected every three hours for a total of

24 hours, and ratios between *CeTOR* isoforms were determined by RT-qPCR as in Figure 4D; error bars represent standard deviation. **F) The timing of spermatogenesis is not affected in *prg-1* or *csr-1* mutants.** Worms were synchronized at L1 stage and grown at 20°C for 42 hours to obtain L4 animals. Some *csr-1(tm892)* mutants showed a developmental delays while others presented canonical L4 features in terms of size and the presence of a white spot (corresponding to an empty uterus) next to the vulva when observed under the stereomicroscope. L4 worms were selected on the basis of these features. **G) Further validation of L4 stage by vulva morphology and presence of the vulval “christmas tree” shape, which is a hallmark of the L4 stage.** DIC microscopy and high magnification of spermatogenesis areas (white boxes) in wild type, *prg-1(tm872)* and *csr-1(tm892)* L4 animals revealed the presence of sperm precursors. White arrows indicate spermatids. **H) DAPI staining of some selected L4 animals (n>10 for each of the three strains).** All animals showed the presence of sperm precursors. Areas within white boxes are shown at high magnification. White arrowheads indicate sperm precursors. White asterisks indicate sperm.

Figure S4



G

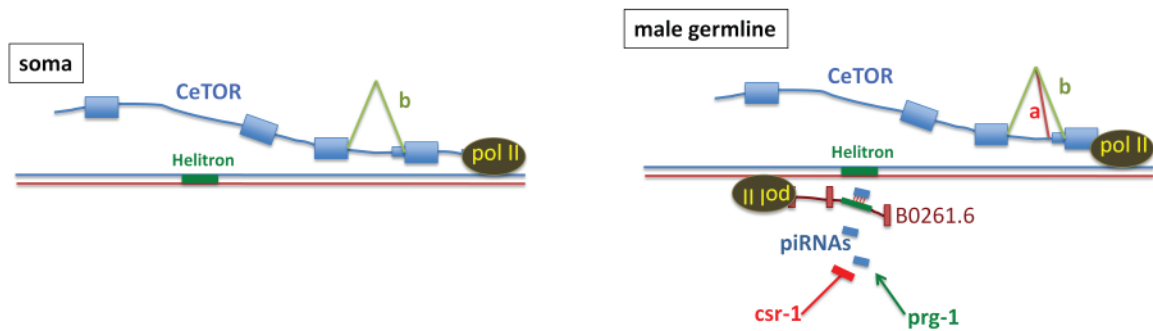


Figure S4. Rescue of the progressive sterility of *prg-1* mutants by dsRNA against intron 21 (related to Figure 4). **A) Progressive sterility of *prg-1* mutants.** Progeny counts were determined for 10 worms in each data point after 10, 15 or 20 generations after receiving the strain from CGC. Error bars represent the standard deviation. **B, C) RNAi rescue experiment controls.** N2 worms were fed for 20 generations on bacteria expressing the corresponding dsRNA clone before counting progeny sizes. Different researchers performed the same experiment twice in different laboratories; the experiment in B) includes i21, i22, and L4440 dsRNA clones; while the experiment on C) includes more dsRNA clones controls as explained below. The experiments in both A and B were performed by feeding *prg-1(tm872)* worms with bacteria expressing dsRNA for 15 generations (Panel B) or for 7 generations (Panel C). We found that optimal rescue of the *prg-1* sterility phenotype by intron 21 dsRNA, required that the *prg-1* worms display a strong phenotype (low progeny counts), but under conditions of extremely low progeny counts intron 21 dsRNA did not rescue the strong sterility phenotype. Thus, the effect of feeding *prg-1* worms with *CeTOR* intron 21 dsRNA can be assimilated to a delay in the progressive sterility phenotype caused by *prg-1* mutation. C) Progeny counts for *prg-1* worms after 7 generations of feeding with the corresponding dsRNA-expressing bacteria (n>5) (* data

from F36A2.10(RNAi) worms corresponds to generation 6, due to sterility at generation 7). F55D12.6, F36A2.10 and T01E8.8 transcripts are highly abundant during spermatogenesis; R04D3.7 and F39C12.3 correspond to genes not expressed in the germline that contain intronic helitrons targeted by the RNAi clones used. B0261.6 appears to be the only helitron-containing transcript expressed in germline. **D) Rescue of *prg-1* mutants by crossing to WT worms.** *prg-1* worms from generations 6 and 21 were crossed to N2 males and the levels of progeny scored. Error bars indicate the standard deviation. **E) Absence of effects on progeny counts of feeding wild-type worms with dsRNA expressing bacteria for 20 generations.** Progeny counts of N2 worms that were fed with the corresponding dsRNA bacteria for 20 generations. Error bars indicate the standard deviation. **F) Progeny levels on transgenic worms with *pie-1::B0261.6* single insertion.** Progeny counts of transgenic worms that overexpress B0261.6 under the *pie-1* promoter, compared to a control strain. Error bars indicate the standard deviation. **G) Model for male germline-specific regulation of *CeTOR* alternative splicing.** In somatic tissues, *CeTOR* pre-mRNAs are spliced to 3' splice site b. Expression of the B026.1 antisense transcript during spermatogenesis offers sequences complementary to piRNAs directed against a Helitron transposon located within the first intron of the antisense transcript. The antagonistic effects of Argonaute proteins PRG-1 and CSR-1 influence piRNA synthesis and/or function, which in turn modulate *CeTOR* expression and activation of 3' splice site a.

Table S1

	Antisense gene	Sense gene	Alt splicing event	Upstream or downstream
1	Y74C10AR.2	<i>abtm-1</i>	cassete exon	downstream
2	Y105E8A.27	<i>catp-1</i>	alt 5' ss	downstream
3	F36A2.10	F36A2.9	cassete exon	downstream
4	F56B3.6	F56B3.4	cassete exon	downstream
5	B0261.6	<i>let-363</i> (TOR)	alt 3' ss	downstream
6	Y53F4A.2	R05H10.3	cassete exon	upstream
7	F55D12.6	<i>unc-55</i>	alt 3' ss	downstream

Table S1. Seven examples of sense/antisense transcript pairs with sperm-specific expression of antisense transcripts and alternative splicing events identified in the sense transcript.

The relative location of the alternatively spliced regions and the site of antisense transcription are also indicated.

Supplementary Materials and Methods

Strains, samples and RNA extractions

Mutant strains: *fem-1 (hc17)*, *fem-3 (q20)*, *him-8 (e1489)*, *prg-1* (WM161) and *csr-1* (WM214) were obtained from the CGC. Synchronized worm samples were obtained by bleaching and the developmental stage was confirmed by microscopy of vulva development (white-crescent stage (1)). For figure S9, white-crescent stage worms were selected and samples collected every 3 hours. Samples from whole worms were obtained from 15 worms; dissected gonads for the RT-PCR assays of figure 2 were collected from 50-100 worms. Purified oocytes were obtained as reported in (2). Purified sperm was obtained from dissected male gonads and isolated on sperm buffer (Shaham, Wormbook). Purified adult males were obtained from a synchronous population of *him-8 (e1489)* males and filtered through a 35µm filter. RNA extractions were performed with Trizol (Invitrogen) and further purified using RNease Plus Micro kit (Qiagen). All samples were collected in at least biological triplicates.

RT-qPCR and semi-qRT-PCR

RT reactions were carried out using Superscript III (Invitrogen) on a 20 µl reaction containing RNA samples obtained either from whole worms, dissected gonads or purified oocytes. cDNA was then diluted 3x and used for qPCR with Sybr Green mix (Applied Biosystems), qPCR reactions were carried out in technical triplicates. Semi-quantitative RT-PCR was performed with Go Taq polymerase (Promega) on a thermocycler for 30 cycles using primers covering the alternative junctions of exons 24 and 25. PCR products were digested with TasI, which recognizes sequences present only in the *CeTORa* isoform, and the products corresponding to the a and b isoforms were resolved by electrophoresis on 6% acrylamide gels.

To normalize for differences in germline production among different mutants, the levels of three sperm-specific markers, *spe-44*, *msp-10* and *spe-26* were measured by RT-qPCR in RNA preparations of whole worms; the average expression of these three markers was used to normalize the expression values of B0261.6, *CeTOR* (expression) or *CeTORa /b* isoforms. The robustness of this normalization approach was validated with consistent results using all possible pair combination of markers (Figure S6).

RNA-Seq

mRNA sequencing libraries for figures 1, S1 and S4 were generated by the dsDNALigSeq method as described in (3). Total RNA was extracted from frozen tissue samples with mirVana (Ambion) and the library was prepared using reagents from Illumina (RS-100-0801). The sequence data is available at the NCBI Gene Expression Omnibus (<http://www.ncbi.nlm.nih.gov/geo/>) under accession no. GSE22410. mRNA and sRNA sequencing libraries for figure S5 were sequenced according to manufacturer recommendations with Truseq kit (Illumina) at the CRG sequencing facility.

***in situ* hybridizations**

In situ hybridization of mRNA in dissected gonads was performed according to the protocol described in (4), although gonad dissection, washes, and incubations were performed on a multi-well Pyrex plate (Electron Microscopy Sciences). Primers employed to generate sense and antisense probes for B0261.6 mRNA correspond to the sequences 5'-TGCTCGCGATAATTCCTCTTCTTC-3' and 5'-CAACGACACTTGCCTCGGCACTA-3',

respectively. The sense probe was used as negative control. Probes were diluted 1:2 prior to the hybridization step.

Phenotypic rescue experiment

Genomic fragments of introns 21 and 22 of *CeTOR* (*let-363*) excluding 40-50bp from the 5' and 3' splice sites were obtained by PCR and cloned into L4440 feeding vector. Clones corresponding to transcripts on Figure S9 were obtained from the *C. elegans* RNAi library (5). For figure S11, N2 worms were fed for 20 generations on bacteria expressing the corresponding dsRNA clone before counting progeny sizes. Figures S11A and S11B correspond to *prg-1*(tm872) worms fed with bacteria expressing dsRNA for 15 generations (Figure S11A) or for 7 generations (Figure S11B). We found that optimal rescue of the *prg-1* sterility phenotype by intron 21 dsRNA, required that the *prg-1* worms display a strong phenotype (low progeny counts), but under conditions of extremely low progeny counts intron 21 dsRNA did not rescue the strong sterility phenotype. Thus, the effect of feeding *prg-1* worms with *CeTOR* intron 21 dsRNA can be assimilated to a delay in the progressive sterility phenotype caused by *prg-1* mutation.

Bioinformatics

mRNA-Seq reads were aligned to the *C. elegans* genome (WS190) using bowtie (6) and tracks were uploaded to the UCSC genome browser for display. To identify differentially expressed antisense transcripts, DEseq (7) was used from the data obtained from bowtie. Previously

reported sRNA-Seq data were retrieved from GSE19414 for *glp-1* mutants and N2 L4 worms (Figure 1c and S3); from GSE11738 for *prg-1* mutants and N2 control worms (Figure 3a); and from GSE18167 for *csr-1* mutant and N2 control worms (Figure 3c). Reads were aligned to the TOR locus using bowtie. Quantification of sRNA reads targeting B0261.6 was carried out using Perl scripts and Excel datasheets. Values displayed in Figure 3 correspond to small RNA reads per million of reads mapped to the entire genome; in the case of small RNA reads targeting intron 1 of B0261.6 (including the Helitron) in Figures 3b and 3e, they include reads uniquely mapped to the intron as well as reads that also map to other Helitrons with identical sequence

Literature cited

1. M. R. Koelle, H. R. Horvitz, *Cell* **84**, 115 (1996).
2. M. A. Miller, *Methods Mol Biol* **351**, 193 (2006).
3. A. T. Lamm, M. R. Stadler, H. Zhang, J. I. Gent, A. Z. Fire, *Genome Res* **21**, 265 (2011).
4. M. H. Lee, T. Schedl, *WormBook*, 1 (2006).
5. R. S. Kamath *et al.*, *Nature* **421**, 231 (2003).
6. B. Langmead, C. Trapnell, M. Pop, S. L. Salzberg, *Genome Biol* **10**, R25 (2009).
7. S. Anders, W. Huber, *Genome Biol* **11**, R106 (2010).